

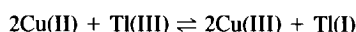
## Calcium and Thallium Nonstoichiometry in the 108 K Superconductor $Tl_2Ba_2CaCu_2O_8$ : HREM Study

M. HERVIEU, C. MARTIN, J. PROVOST, AND B. RAVEAU

*Laboratoire de Cristallographie et Sciences des Matériaux, CRISMAT, ISMRa, Université de Caen, Bd du Maréchal Juin, 14032 Caen Cedex, France*

Communicated by J. M. Honig, July 23, 1988

The calcium and thallium nonstoichiometry in the 108 K superconductor  $Tl_2Ba_2CaCu_2O_8$  was studied by high-resolution electron microscopy. It is shown that deviations from stoichiometry correspond to intergrowth phenomena. The rock salt-type layers are often affected. One indeed observes thallium monolayers which correspond to the replacement of the triple rock salt-type layer  $[(TlO)_2(BaO)_2]$  by a double rock salt-type layer  $[(TlO)(BaO)_2]$ , i.e., to extended defects of formulation  $TlBa_2CaCu_2O_7$ , member  $n = 2$  of the series  $(AO)_n(A'CuO_{3-y})_m$ . Intercalation of additional  $[CaO]_\infty$  layers in the rock salt-type layers is also observed, which lead to quintuple layers  $[(BaO)_2(TlO)_2(CaO)_2]$ . Extended defects corresponding to the replacement of one calcium layer by a thallium layer in the double oxygen-deficient perovskite layers are also observed. Attention is drawn to the fact that such defects may affect the dynamical equilibrium:



and also change the Cu(III) content by modification of the charge balance. © 1988 Academic Press, Inc.

The study of copper thallium oxides has allowed new high- $T_c$  superconductors to be isolated with critical temperatures ranging from 75 to 125 K (1–10). The structural analysis of those oxides allows a general formula (1)  $(AO)_n(A'CuO_{3-y})_m$  to be established which represents the intergrowth of multiple rock salt-type layers  $[AO]_\infty$  ( $A = Ba, Tl$ ) with multiple oxygen-deficient perovskite layers  $[A'CuO_{3-y}]_m$  ( $A' = Ba, Ca$ ). The oxygen and cationic deviation from stoichiometry is a problem of major importance in those oxides for the understanding of their superconducting properties.

For example, the superconducting properties of the “2212” oxide,  $Tl_2Ba_2CaCu_2O_8$ , whose structure (Fig. 1) has previously been studied (3–4) can be explained in different ways. In a first approach, this 108 K superconductor can be considered rigorously stoichiometric, so that the mixed-valence Cu(III)–Cu(II) necessary for the appearance of superconductivity would be induced by a dynamical exchange between thallium and copper according to the equilibrium  $2Cu(II) + Tl(III) \rightleftharpoons 2Cu(III) + Tl(I)$ ; in this first hypothesis the thallium layer would play the role of a reservoir of holes. A second plausible model which

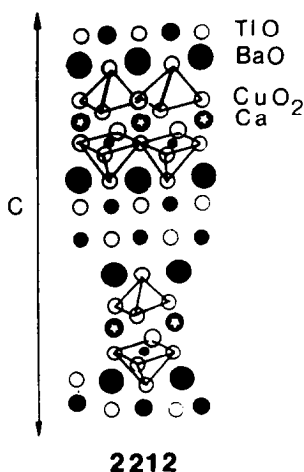


FIG. 1. Idealized drawing of  $Tl_2Ba_2CaCu_2O_8$  structure;  $n = 3$  and  $m = 2$ .

would explain the mixed valence of copper deals with either an oxygen excess stoichiometry leading to the formulation  $Tl_2Ba_2CaCu_2O_{8+\delta}$ , or with a cationic nonstoichiometry involving thallium, barium, or calcium. From this it is clear that the understanding of superconductivity in this oxide requires a thorough investigation of the homogeneity of the samples. This paper deals with the HREM study of a "2212" oxide.

### Experimental

The sample was prepared as previously reported (5) from a stoichiometric mixture of  $Tl_2O_3$ ,  $BaO_2$ ,  $CaO$ , and  $CuO$  pressed in a form of pellet and heated in a sealed quartz tube. The X-ray analysis led to a pure tetragonal phase with  $a = 3.86 \text{ \AA}$  and  $c = 29.388 \text{ \AA}$ ; the dc resistance measurements yielded superconducting behavior with a midpoint  $T_c$  of 108 K. The X-ray powder data clearly show thallium nonstoichiometry and the possibility of partial occupancy of calcium sites by a heavier cation which was assumed to be thallium, based on ion size considerations (4). The occupancy fac-

tor of the oxygen site localized in the calcium plane, i.e., between the  $CuO_5$  pyramids, was refined to 0.0.

The HREM study was performed on a JEOL 200 CX electron microscope, operating at 200 kV, and the image calculations were carried out with a multislice program, using the X-ray powder data.

### Results

The interpretation of the variations in the image contrast in terms of nonstoichiometric features needs a correlation between

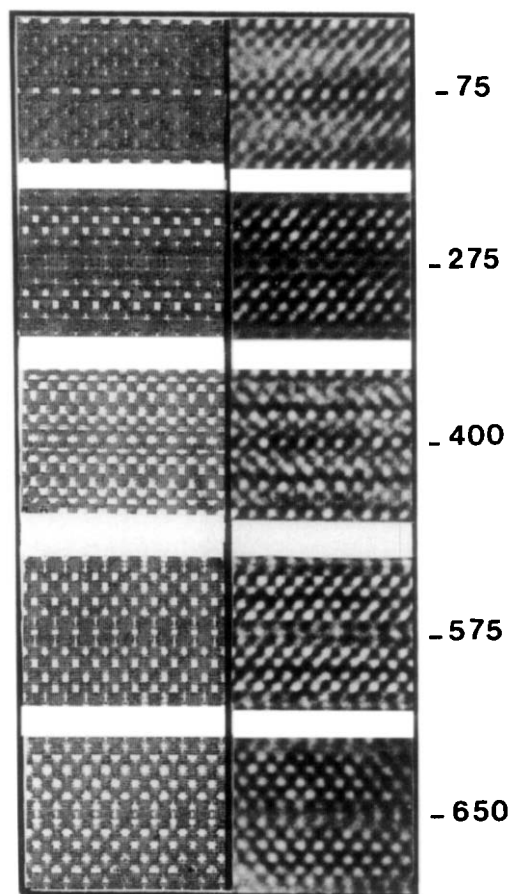


FIG. 2. Example of the experimental and calculated images. The structural parameters are those of Ref. (4);  $C_s = 0.8 \text{ mm}$ , 139 beams, crystal thickness =  $30.9 \text{ \AA}$ ,  $\alpha/2 = 0.8 \text{ mrad}$ , focus spread =  $150 \text{ \AA}$ , and voltage = 200 kV; the focus values are given in angstroms.

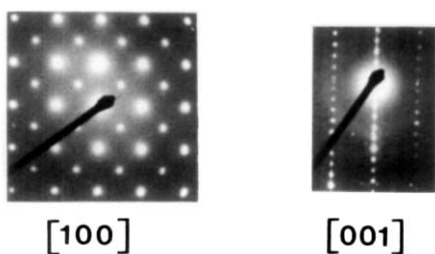


FIG. 3. [100] and [001] electron diffraction patterns.

every image and the projected potential. This was achieved through the comparison between the experimental through-focus series and the calculated images for various crystal thicknesses. Some examples are

given in Fig. 2. These images confirm the "intuitive" interpretation which was the basis of our structural model. Thus, for a focus value of 400 Å, the white dots of the image 2 can be correlated with the oxygen positions. Conversely, for a focus value close to -650 Å, the white dots correspond to the cation positions (except calcium) in the same image 2. In that case, the barium and thallium rows appear, in a striking way, as four rows of shifted bright spots.

The investigation of the crystals showed that [001] images cannot yield significant information on nonstoichiometry, owing to the projection of the anions and cations along the *c* axis. On the contrary, [100] im-

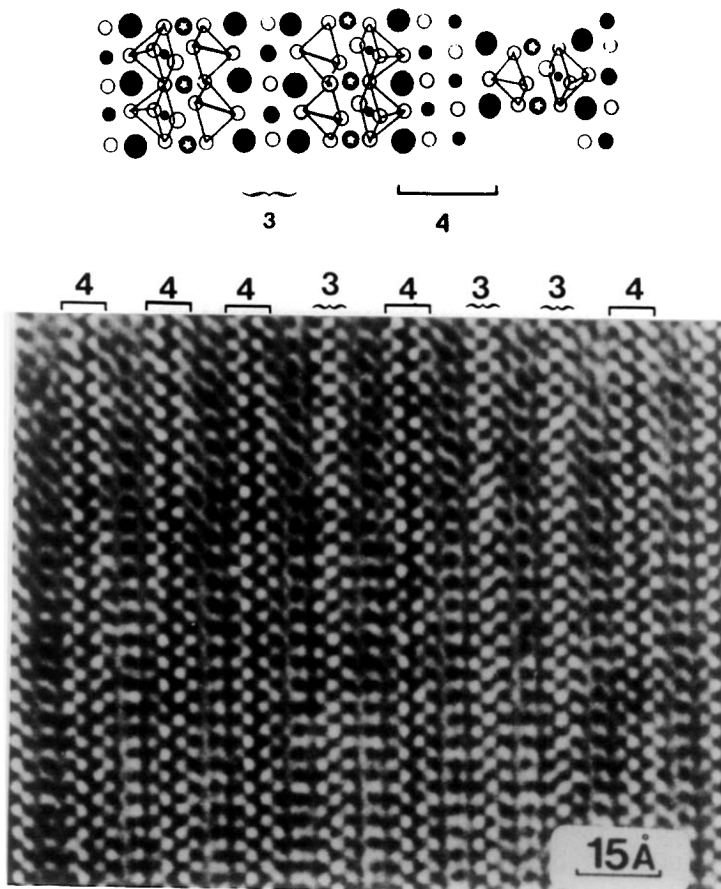
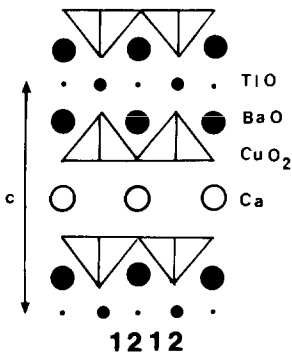


FIG. 4. Defect in rock salt-type layers:  $[(\text{BaO})_2(\text{TlO})]$  layers appear in a  $[(\text{BaO})_2(\text{TlO})_2]$  matrix; they are noted 3 and 4, respectively.

FIG. 5.  $\text{TlBa}_2\text{CaCu}_2\text{O}_7$  structure.

ages provide essential information. It was previously reported (10) that streaks are observed along  $c^*$  on some [100] electron diffraction patterns (Fig. 3). It appears from the observation of the corresponding HREM images that these features are mainly correlated with the existence of defects in the rock salt-type layers.

The far more numerous defects which affect the AO layers are presented in Fig. 4 and were previously reported (10). The contrast of this image corresponds to a focus value where the cation positions are

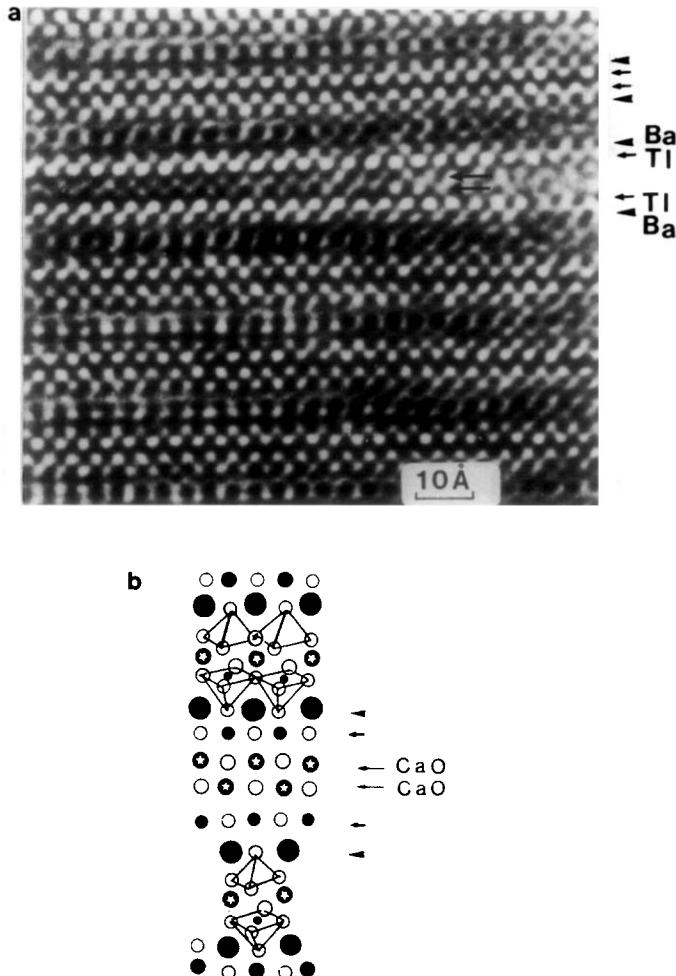


FIG. 6. (a) Intercalation of (CaO) layers between the (TlO) layers. (b) Idealized model of the defect structure.

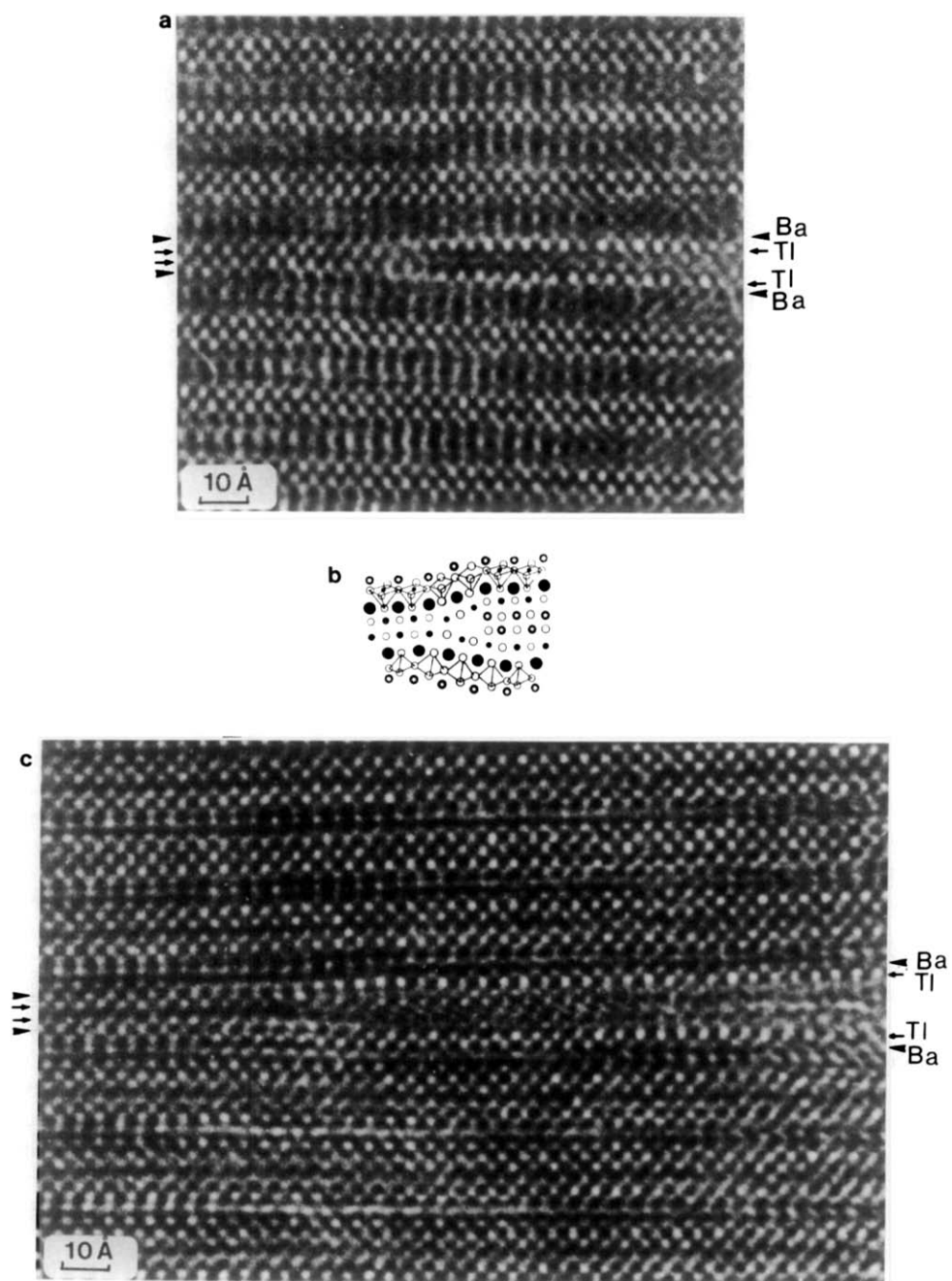


FIG. 7. (a) The additional (CaO) layers can be interrupted in the bulk. (b) Idealized model of the phenomenon. (c) Example of a larger (CaO) layer.

highlighted. The rock salt-type layers appear clearly to be made up either of four  $[AO]_{\infty}$  or of three  $[AO]_{\infty}$  rows ( $A = \text{Ba}, \text{Tl}$ ); the local sequence is 4-*P*-4-*P*-3-*P*-4-*P*-3-*P*-3-*P*-4-*P*-4-*P*, where the numbers 4 and 3 correspond to  $[(\text{BaO})_2(\text{TlO})_2]$  layers and  $[(\text{BaO})_2(\text{TlO})]$  layers, respectively, and where *P* represents the double oxygen-deficient perovskite layer  $[\text{CaCu}_2\text{O}_5]_{\infty}$ . This feature can be described by the disappearance of one TlO layer: this would correspond to a "Ba-Tl-Ba" sequence of the *A* cations for a triple row, instead of the sequence of four cations "Ba-Tl-Tl-Ba" in the normal "2212" matrix. Alternatively, this defect can be expressed as the occurrence of an  $n = 2$  member of composition  $\text{TlBa}_2\text{CaCu}_2\text{O}_7$  in an  $n = 3$  matrix (Fig. 5); such an observation leads to the characterization of a new thallium family, namely  $[(\text{BaO})_2(\text{TlO})][A'\text{CuO}_{3-y}]_m$  (7-10).

The second type of defect which affects the NaCl layers corresponds to the intercalation of additional  $[AO]_{\infty}$  layers into their mid position as shown in Fig. 6. Considering that the images where the cations appear as white dots are the best for such an interpretation, we observe clearly six rows of shifted white dots with the following intensities: two bright, two weak, and two bright. Such intermediate rows are assumed to correspond to two additional rock salt-type layers: their weak contrast is in agreement with the presence of calcium oxygen  $[\text{CaO}]_{\infty}$  layers (Fig. 6b).

These additional  $[\text{CaO}]_{\infty}$  layers can be infinite (Fig. 6a) or can be interrupted as shown in Fig. 7. In this latter case, the NaCl-type layers are clearly visible even in the thick part of the crystal where a normal sequence is observed, whereas on the edge of the crystal two additional rows are observed. More than two rows are sometimes intercalated, as shown in Fig. 7c.

Another defect is observed in Fig. 8, where the focus value is assumed to be close to  $-650 \text{ \AA}$ , i.e., where the white dots

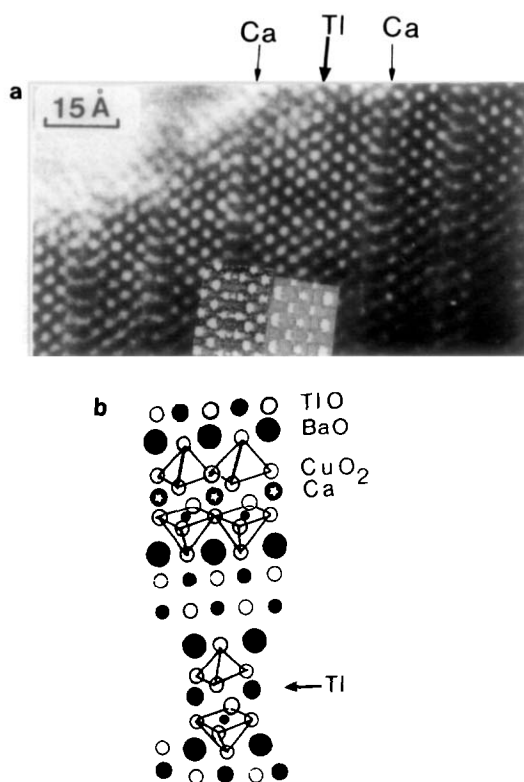
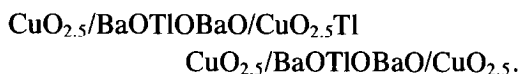


FIG. 8. (a) Experimental image of a stacking defect. This is assumed to correspond to the replacement of a Ca row by a Tl row, in agreement with the calculated images of both layers superimposed with the experimental image. (b) Idealized model of such a defect in a "2212" matrix.

are correlated with the positions of the cations, except for the calcium ions. The normal sequence is thus of six rows of white spots, corresponding to the sequence: "Cu-Ba-Tl-Tl-Ba-Cu." The defect appears as eleven adjacent rows of shifted white spots. A careful examination of these images and especially of the distances between the rows shows that these defects cannot simply be interpreted as a thicker rock salt-type multilayer, but correspond to a double defect: the bright contrast of the middle row suggests that a calcium layer is replaced by a thallium layer (Fig. 8b) leading to a double perovskite layer  $[\text{TlCu}_2\text{O}_5]_{\infty}$ ; the latter is sandwiched between two

thallium-deficient rock salt-type layers  $[(\text{BaO})_2(\text{TlO})]$  ( $n = 2$ ). Calculated images of the two perovskite-type layers,  $[\text{CaCu}_2\text{O}_5]_\infty$  and  $[\text{TlCu}_2\text{O}_5]_\infty$ , are superimposed with the experimental image; the difference in contrast of the Ca row (very weak dots) and the Tl row (white dots) is well shown in both images. The sequence of the eleven rows can thus be represented as:



This interpretation is in agreement with the double nonstoichiometry on thallium and calcium observed from X-ray powder data.

The present results show that the deviation from stoichiometry for thallium and calcium which can be observed by X-ray diffraction (3–4) results from intergrowth phenomena which affect the rock salt-type layers. Consequently, this deviation from stoichiometry may play an important role in the superconducting properties of those oxides: It can indeed increase the Cu(III) content by changing the charge balance in the bulk, but it can also affect the thallium layers and thus influence the role of hole reservoir of such layers. The synthesis of "2212" oxides by different methods—changing the nominal composition and the thermal treatment—leads to oxides which appear as pure phases from X-ray diffraction analysis but which exhibit different physical properties (11). The analysis of these phases by high-resolution electron microscopy, with the particular aim of characterizing the nonstoichiometry fea-

tures, may yield essential information on the correlation between the microstructures and the superconducting behavior; this work is in progress.

## References

1. Z. Z. SHENG, A. M. HERMAN, A. EL ALI, C. ALMASAN, AND T. DATTA, *Phys. Rev. Lett.*, in press; *Nature (London)*, in press.
2. R. M. M. HAZEN, D. W. FINGER, R. J. ANGEL, C. T. PREWITT, AND C. C. HAIDYACOS, *Phys. Rev. Lett.*, to be published.
3. M. A. SUBRAMANIAN, J. C. CALABRESE, C. C. TORARDI, J. GOPALAKRISHNAN, T. R. ASKEV, R. B. FLIPPEA, K. J. MORRISSEY, Y. CHONDHRY, AND A. W. SLEIGHT, *Nature (London)* **332** (1988).
4. A. MAIGNAN, C. MICHEL, M. HERVIEU, C. MARTIN, D. GROULT, AND B. RAVEAU, *Mod. Phys. Lett. B* **2**(5), 681 (1988).
5. M. HERVIEU, C. MICHEL, A. MAIGNAN, C. MARTIN, AND B. RAVEAU, *J. Solid State Chem.* **74**, 428 (1988).
6. S. PARKIN, V. Y. LEE, E. M. ENGLER, A. I. NAZZAL, J. C. HUANG, G. GORMAN, R. SAVOY, AND R. BEYERS, *Phys. Rev. Lett.*, in press.
7. C. MARTIN, C. MICHEL, A. MAIGNAN, M. HERVIEU, AND B. RAVEAU, *C.R. Acad. Sci.* **11**, 4 (1988).
8. S. S. P. PARKIN, V. Y. LEE, A. I. NAZZAL, R. SAVOY, R. BEYERS, AND S. I. LA PLACA, submitted for publication.
9. M. A. SUBRAMANIAN, J. C. CALABRESE, C. C. TORARDI, J. GOPALAKRISHNAN, T. R. ASKEV, R. B. FLIPPEN, K. J. MORRISSEY, U. CHOWDRI, AND A. W. SLEIGHT, *Nature (London)* **332**, 420 (1988).
10. M. HERVIEU, A. MAIGNAN, C. MARTIN, C. MICHEL, J. PROVOST, AND B. RAVEAU, *J. Solid State Chem.* **75**, 212 (1988).
11. B. RAVEAU, C. MICHEL, M. HERVIEU, F. DESLANCES, AND A. MAIGNAN, in "Proceedings of the International Conference on the First Two Years of High  $T_c$  Superconductivity, 6 May 1988, Tuscaloosa, Alabama" (1988).